Operator evolution from the similarity renormalization group and the Magnus expansion

A. J. Tropiano[1], S. K. Bogner[2], R. J. Furnstahl[1]

[1] *Department of Physics, The Ohio State University, Columbus, OH 43210, USA*

[2] *National Superconducting Cyclotron Laboratory and Department of Physics and Astronomy, Michigan State University, East Lansing, MI 48824, USA*

(Dated: September 19, 2019)

Abstract

Ideas for Magnus / SRG operator evolution paper

– SRG/Magnus evolution in different potentials (non-local, local, semi-local). Universality. High cutoffs.

– Block-diagonal generator for high cutoff potentials and operator evolution. How the block-diagonal generator handles spurious bound states.

– Testing the Magnus expansion for high cutoff potentials using the potentials from Wendt 2011 for comparison. Spurious bound states and connection to intruder states in IMSRG calculations.

– Operator evolution for different potentials and generators.

I.   INTRODUCTION

Background on modern nuclear potentials.

– Wide range of NN potentials.

- Chiral EFT background.

- Different potentials but give same S-matrix.

– Implementation to many-body calculations and SRG decoupling.

- Strong coupling between low- and high-momentum matrix elements in NN potentials.

- Very difficult to implement these interactions in many-body methods using basis expansions. Matrix dimension becomes too large for accurate calculations.

- RG transformations are used to soften the interaction to make many-body methods feasible. One such method, the SRG, also preserves observables from unitarity.

- How do different potentials change under SRG transformations?

SRG formalism

– The SRG decouples low- and high-momentum scales by applying a continuous unitary transformation $U(s)$ where $s = 0 \to \infty$ is the flow parameter.

– The 'dressed' or evolved operator is given by

$$O(s) = U(s)O(0)U^{\dagger}(s), \tag{1}$$

where $O(0)$ corresponds to the 'bare' operator.

– Because $U(s)$ is unitary, the observables of the operator are preserved.

– In practice, the unitary transformation U(s) is not explicitly solved for; the evolved operator is given by a differential flow equation which is obtained by taking the derivative of Eqn. (1),

$$\frac{dO(s)}{ds} = [\eta(s), O(s)], \tag{2}$$

where $\eta(s) = \frac{dU(s)}{ds}U^{\dagger}(s) = -\eta^{\dagger}(s)$ is the anti-hermitian SRG generator.

– The generator is defined as a commutator, $\eta(s) = [G, H(s)]$, where G specifies the type of flow or form of the decoupled operator.

– By setting $G = H_D(s)$, the diagonal of the Hamiltonian, the operator is driven to band-diagonal form.

– This choice was implemented by Wegner in condensed matter physics [1].

– In a similar option used in nuclear physics, G is set to the relative kinetic energy, T_{rel}, which also drives to band-diagonal form.

– It is convenient to define $\lambda \equiv s^{-1/4}$ which roughly measures the width of the band-diagonal in the decoupled operator.

– For block-diagonal decoupling, denoted $G = H_{BD}(s)$, the operator is split into low- and high-momentum sub-blocks by specifying a separation in momentum Λ_{BD}.

– These transformations are similar to V_{lowk} Lee-Suzuki transformations but keep the high-momentum matrix elements non-zero, although entirely decoupled from the low-momentum sub-block.

– Generally the flow equation (2) is solved up to some finite value of s with a high-order ODE solver.

– For notational convenience, we write the generators without the s dependence in the rest of the paper.

Universality

– The explicit long-range physics should be the same. Decoupling low- and high-energy gives matching low-energy matrix elements. In the NN potential, this means softened NN interactions should have the same low-momentum matrix elements after sufficient decoupling.

– Add takeaways from Dainton: phase shift equivalence implies matrix element equivalence for λ approaching the momenta of phase equivalence. Correct binding energy is critical or the lowest matrix elements will not match.

– Motivate long list of unaddressed questions: regulator, generator dependence, high cutoffs, the Magnus expansion.

- Regulator. Functional dependence of regulator. Reasons for implementing each.

- Generators. Band- and block-diagonal transformations.

- High cutoffs. Cite Nogga, Wendt, and Tews papers.

- The Magnus expansion. High cutoffs and connection to IMSRG intruder state problem.

Operator evolution

– State how a potential and wave function changes: how does this affect other operators?

– Operator evolution for different potentials (regulators, chiral order, etc.)

– How operators evolve from band- and block-diagonal SRG transformations.

Overview of sections.

II.   SRG EVOLUTION OF NN POTENTIALS

General outline of the section

– Comparison of potential evolution with different regulators, orders, generators.

– Universality.

– Discussion of high cutoffs, block-diagonal generator at high cutoffs, and how it handles spurious bound states.

– Use high cutoffs to transition to Magnus test problem.

Analysis of figures

– Fig. 1 illustrates the SRG in a nutshell. Here, we evolve three partial wave channels of RKE N^{3}LO [2] where the cutoff $\Lambda = 450$ MeV to $\lambda = 1.5$ fm^{-1}. We see that the off-diagonal elements of the potential approach zero and the potential is driven to band-diagonal form.
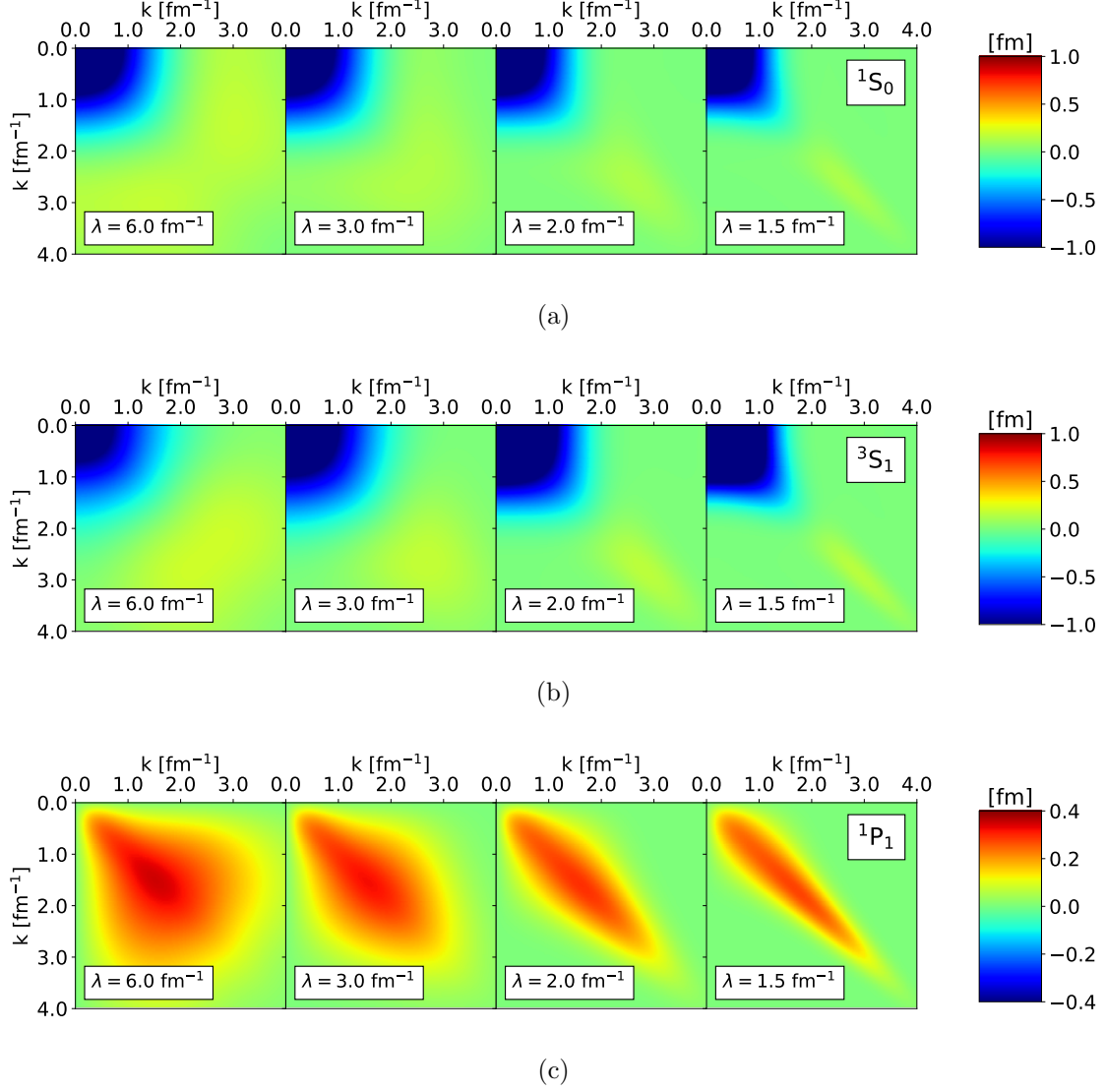
FIG. 1: Matrix elements of the RKE N³LO potential SRG-evolving in λ right to left under transformations with the Wegner generator in the $^1S_0$ (a), $^3S_1$ (b), and $^1P_1$ (c) channels.

– In Fig. 2 we consider three different SRG-evolved potentials in the $^3S_1$ channel: EM N³LO (500 MeV cutoff) [3], RKE N³LO (450 MeV cutoff) [2], and Gezerlis et al. N²LO (1 fm cutoff) [4]. The major difference in these three potentials are the regulator functions in the contact and pion-exchange terms. The EM N³LO interaction is a non-local potential where both contact and pion-exchange interactions feature a non-local regulator function of the form $\exp[-(p/\Lambda)^{2n} - (p'/\Lambda)^{2n}]$, where Λ is the momentum-space cutoff and n is an integer. However, a non-local regulator function for pion-exchange contributions can introduce regulator artifacts for cutoffs Λ lower than the breakdown scale Λ_b. Several semi-local

chiral potentials have been introduced to reduce regulator artifacts, such as the RKE N^{3}LO potential. Here, a local regulator function is applied for the long-range interactions in momentum-space, while a non-local regulator function is used for the short-range interactions. In some instances, non-local interactions are not suitable for *ab initio* approaches such as the quantum Monte Carlo (QMC) method motivating the need for fully local potentials. The Gezerlis et al. N^{2}LO potential is an example of a local interaction where the long-range terms have a local regulator function in coordinate-space and the short-range terms have a local regulator function in momentum-space.

– Takeaways from Fig. 2: completely different at $\lambda = 6$ fm^{-1} but low-momentum matrix elements are similar at $\lambda = 1$ fm^{-1}. Decoupled, low-momentum matrix elements are necessarily the same since the pion-exchange terms are calculated explicitly. (Cutoff dependence can play a role though for lower cutoffs.)
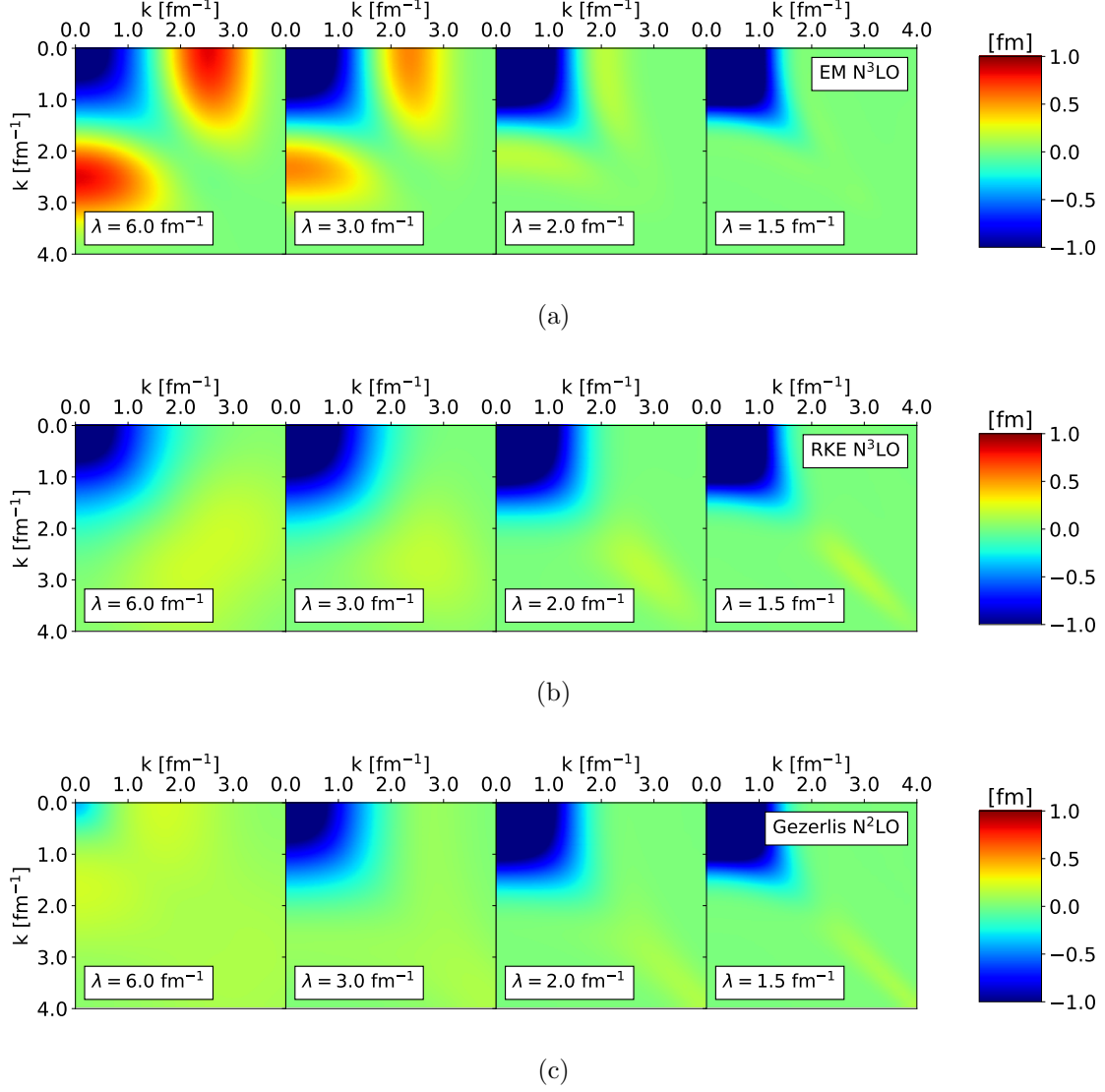
FIG. 2: Matrix elements of the EM N^{3}LO (a), RKE N^{3}LO (b), and Gezerlis et al. N^{2}LO (c) potentials SRG-evolving in λ right to left under transformations with the Wegner generator in the ^{3}S$_1$ channel.

– Fig. 3 shows the SRG-evolved RKE N^{3}LO (450 MeV cutoff) potential in the ^{3}S$_1$ channel for two SRG generators: the Wegner and block-diagonal generators which drive the potential to band- and block-diagonal form, respectively. We continue to evolve to band-diagonal form with respect to the parameter λ, but for the block-diagonal generator, we label sub-plots with the parameter Λ which characterizes the sharp cutoff in decoupling the low- and high-momentum matrix elements.

– Takeaways from Fig. 3: smooth decoupling for Wegner and sharp for block-diagonal, each

unique generator should have its own type of universality. Check this more quantitatively by comparing matrix element "slices".
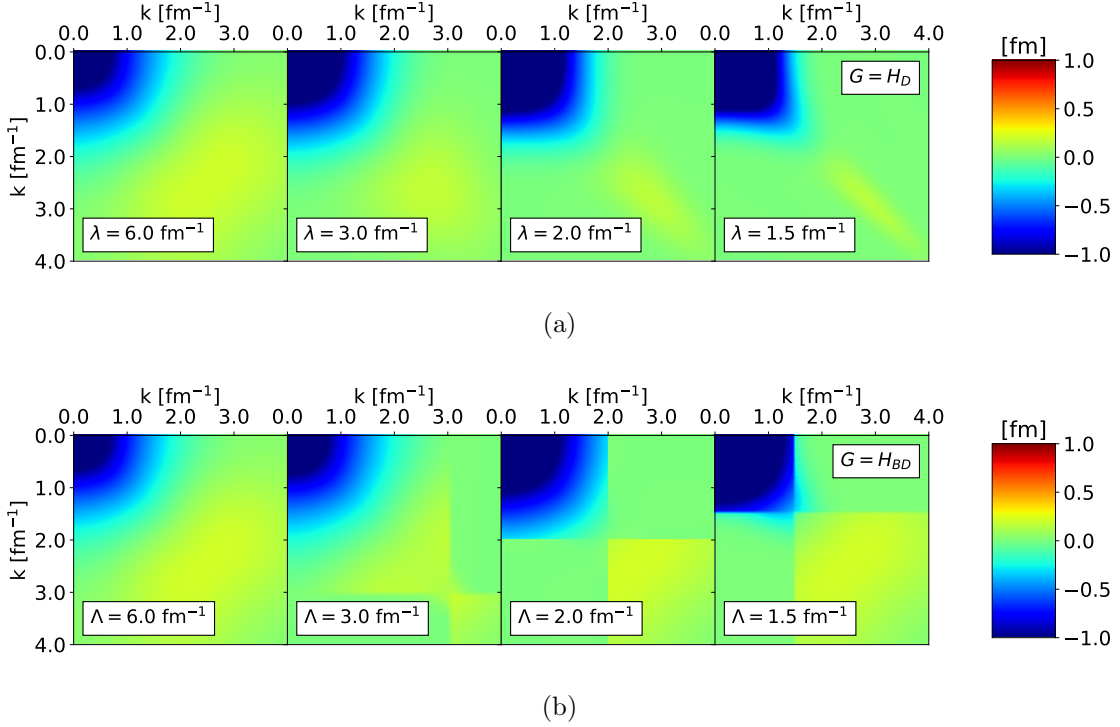

(a)

(b)

FIG. 3: Matrix elements of the RKE N^{3}LO potential SRG-evolving right to left under transformations with Wegner (a) and block-diagonal (b) generators in the ^{3}S$_1$ channel. Here, we use λ for Wegner evolution in the top row and Λ for block-diagonal evolution in the bottom row. For block-diagonal evolution, we fix $\lambda = 1.5$ fm^{-1}.

– Fig. 4 shows the NN phase shifts of EM N^{3}LO, RKE N^{3}LO, and Gezerlis et al. N^{2}LO potentials in the ^{1}S$_0$, ^{3}S$_1$, and ^{1}P$_1$ channels. In [5], it was found that phase equivalence up to some value of momentum k implies matrix element equivalence up to the same value of k in SRG-evolved potentials. We verify this conclusion by checking the matrix elements in Fig. 5 where we see a collapse of the different potential matrix elements to the same line in the last column ($\lambda = 1$ fm^{-1}). Note, Figs. 5-7 show both Wegner and block-diagonal evolution where the solid lines correspond to the Wegner generator and dash-dotted to block-diagonal evolution. We see each generator collapses the potential to a different form because the low- and high-momentum matrix elements decouple in a different manner.

– In the ^{3}S$_1$ channel, we see a slight deviation in the lowest momentum potential matrix element from EM N^{3}LO and the other two potentials. This is due to a minor difference in

the deuteron binding energy ($\approx 1\%$ difference).

– The bottom row of Fig. 7 shows $V(k, 0.5)$ instead of $V(k, 0)$ because the far off-diagonal matrix elements in the ${}^1P_1$ channel are all zero.
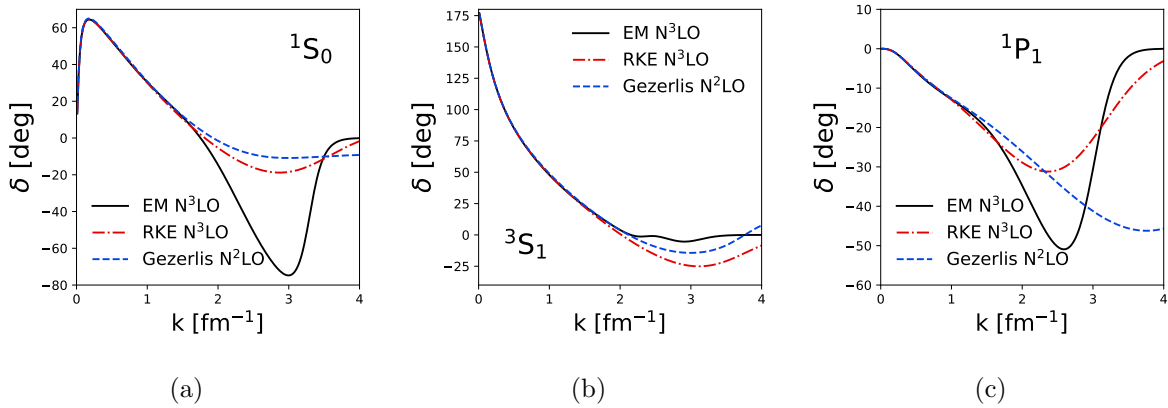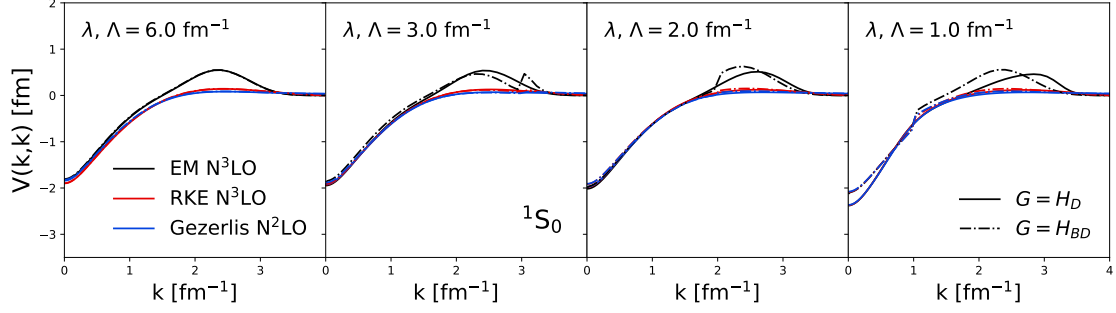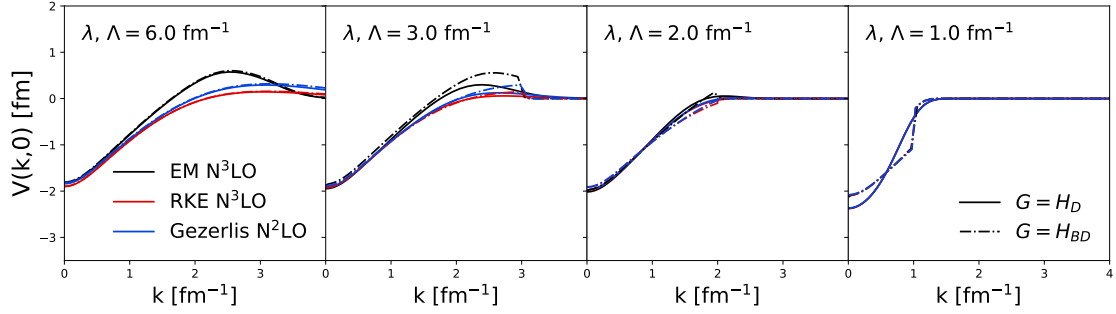

FIG. 4: ${}^1S_0$ (a), ${}^3S_1$ (b), and ${}^1P_1$ (c) phase shifts for the EM N^{3}LO (solid black), RKE N^{3}LO (red dash-dotted), and Gezerlis et al. N^{2}LO (blue dashed) potentials.

(a)

(b)

FIG. 5: Diagonal (a) and far off-diagonal (b) matrix elements of the EM N^{3}LO (black), RKE N^{3}LO (red) and Gezerlis et al. N^{2}LO (blue) potentials SRG-evolving right to left under transformations with Wegner (solid) and block-diagonal (dash-dotted) generators in the ^{1}S$_0$ channel. Here, we use λ for Wegner evolution and Λ for block-diagonal evolution. For block-diagonal evolution, we fix $\lambda = 1$ fm^{-1}.
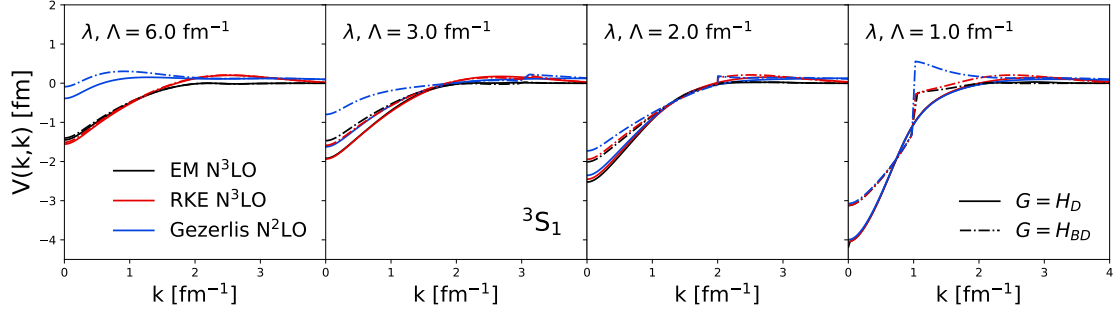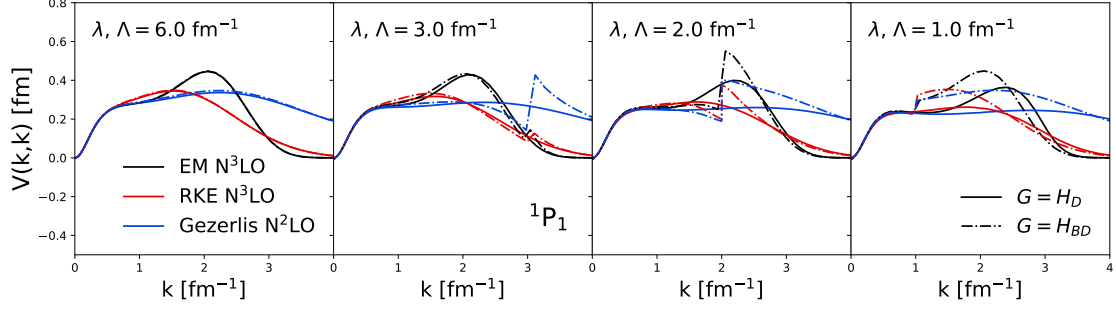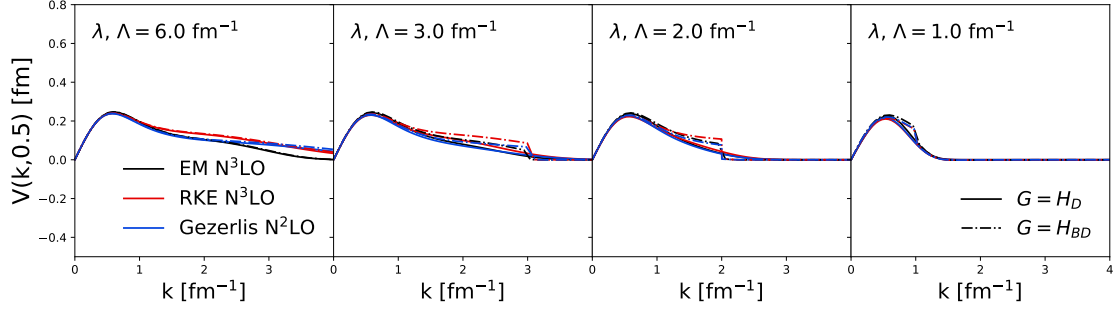
(a)
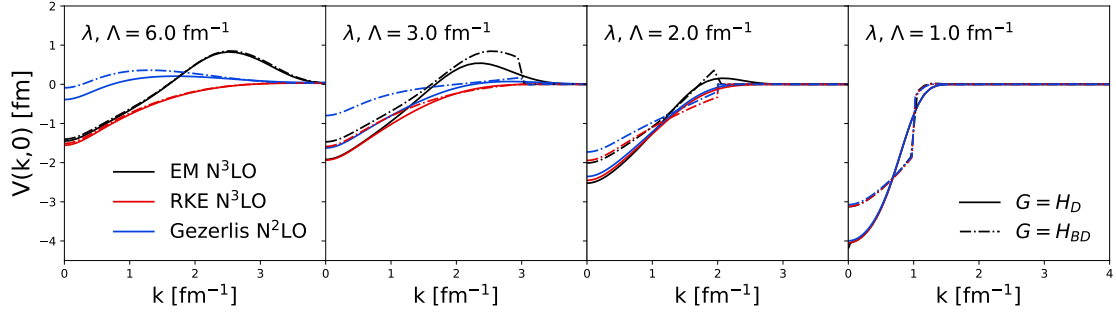
(b)

FIG. 6: Same as Fig. 5 but in the $^3S_1$ channel.

(a)

(b)

FIG. 7: Same as Figs. 5 and 6 but in the $^1P_1$ channel.

High cutoffs

- Cutoff dependence in non-local LO (Wendt) potential.

- Band- and block-diagonal evolution and universality. Add figure analogous to Fig. 6 but for $\Lambda = 4$, 9, and 20 fm^{-1}.

- Spurious bound state(s).

- Discussion on how the block-diagonal generator handles spurious bound states. Where they are "decoupled" in the matrix compared to Wegner.

- Transition to Magnus expansion.

III.   THE MAGNUS EXPANSION

– Connection to IMSRG intruder state.

A.   Formalism

– Motivation: simplifies computational problem for evolving multiple operators, exact unitarity.

– We now consider the Magnus implementation.

– Mathematically speaking, the Magnus expansion is a method for solving an initial value problem associated with a linear ordinary differential equation (ODE).

– Formal details of the Magnus expansion are discussed in [6].

– We will introduce the Magnus expansion in the context of SRG evolving any operator.

– In an intermediate step in deriving Eqn. (2), we have a linear ODE for $U(s)$,

$$\frac{dU(s)}{ds} = \eta(s)U(s). \tag{3}$$

– Magnus showed that one can solve the following equation with a solution $U(s) = e^{\Omega(s)}$ where $\Omega(s)$ is expanded as a power series, $\sum_n^\infty \Omega_n$ (referred to as the Magnus expansion or Magnus series).

– The terms of the series are given by integral expressions involving $\eta(s)$ (again, see [6, 7] for details).

– For our case, we focus on the formally exact derivative of $\Omega(s)$,

$$\frac{d\Omega(s)}{ds} = \sum_{k=0}^\infty \frac{B_k}{k!} ad_\Omega^k(\eta), \tag{4}$$

where B_k are the Bernoulli numbers, $ad_\Omega^0(\eta) = \eta(s)$, and $ad_\Omega^k(\eta) = [\Omega(s), ad_\Omega^{k-1}(\eta)]$.

– We integrate this differential equation to find $\Omega(s)$ and evaluate the unitary transformation directly.

– Then the evolved operator can be evaluated with the BCH formula:

$$O(s) = e^{\Omega(s)} O e^{-\Omega(s)} = \sum_{k=0}^\infty \frac{1}{k!} ad_\Omega^k(O). \tag{5}$$

– As $k \to \infty$ in both sums in Eqns. (4) and (5) the Magnus transformation matches the SRG transformation exactly.

– We investigate several truncations k_{max} in Eqn. (4) and take many terms, $k_{max} \sim 25$, in Eqn. (5).

– Here or earlier (for the following bullets)? Better to motivate the Magnus in the introduction or easier to explain given mathematical detail?

– There are significant advantages in the Magnus implementation.

– In the typical approach, the numerical error associated with solving the flow equation affects the accuracy of the observables for the evolved operator.

– Therefore, one must use a high-order ODE solver in integrating the flow equation (2).

– In the Magnus implementation, unitarity is guaranteed by the form of $U(s)$; in fact, one could solve Eqn. (4) with a simple first-order Euler step-method keeping the same observables while decoupling the operator as desired.

– This offers a decent computational speed-up by avoiding a high-order solver.

– In this paper, we demonstrate this advantage by applying the Magnus implementation using the first-order Euler step-method.

– The second major advantage involves the evolution of multiple operators.

– In many other situations, one may be interested in evolving several operators at a time.

– In the SRG procedure, we would have another set of coupled equations in Eqn. (2), drastically increasing memory usage.

– Each additional operator increases the set of equations - say N equations - by another factor of N.

– In the Magnus, one only needs $\Omega(s)$ to consistently evolve several operators.

– We avoid the cost in memory by directly constructing $U(s) = e^{\Omega(s)}$.

– This is especially useful in IMSRG calculations where the model space can be very large.

– In the next section, we discuss results from Magnus-evolved large-cutoff potentials focusing on the flow of the potential, observables, and operator evolution.

B.   Results

– Comparison to Wendt problem.

– Implications for IMSRG.

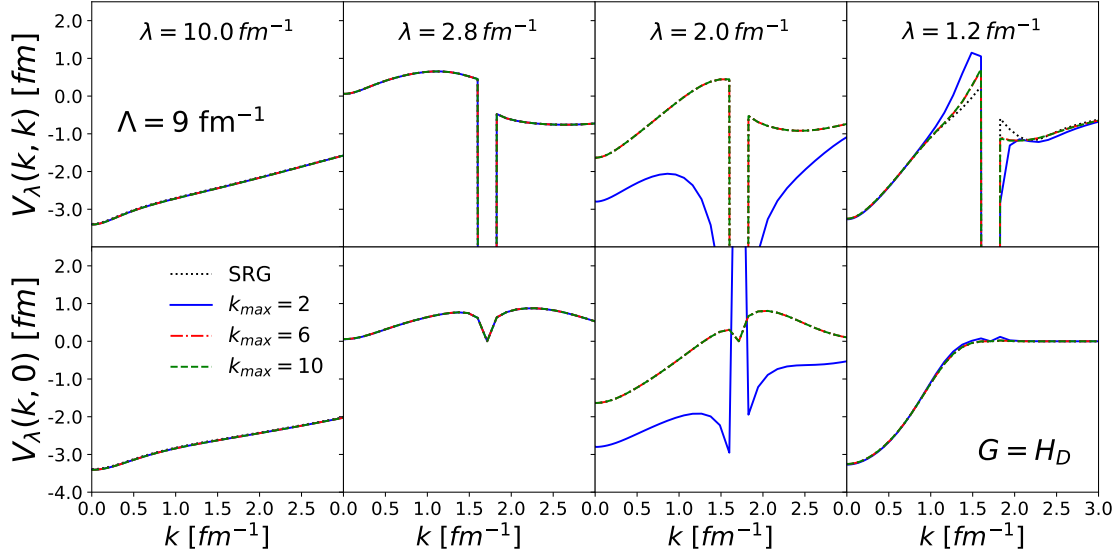– Use discussion of operator evolution to transition to next section.
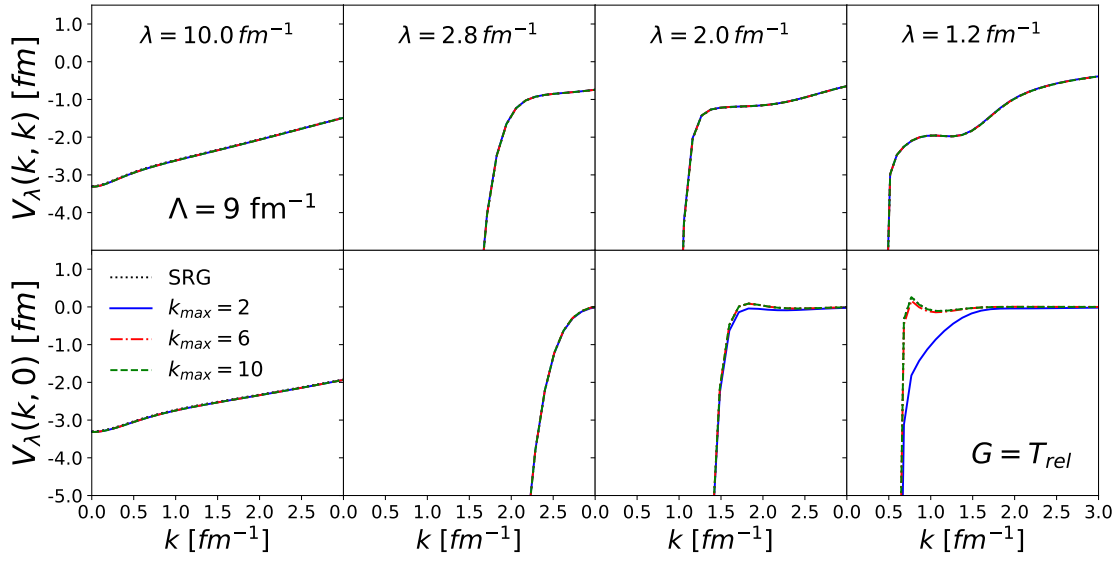
FIG. 8: Caption.

FIG. 9: Caption.

IV. EVOLUTION OF OTHER OPERATORS

– SRG operator evolution for different potentials and generators.

A. Building SRG unitary transformations

Diagonalize initial and evolved Hamiltonians which we will call $H(0)$ and $H(s)$, respectively. This gives $\psi_\alpha(0)$ and $\psi_\alpha(s)$ for each eigenvalue indexed by α. Then the SRG unitary transformation can be computed by taking a sum over outer products of the evolved and initial wave functions:

$$U(s) = \sum_{\alpha=1}^{N} |\psi_\alpha(s)\rangle \langle \psi_\alpha(0)|, \tag{6}$$

where N is the dimension of the Hamiltonian matrix. Here the weights are factored into the wave functions, thus $U(s)$ is unitless.

To evolve operators, we simply apply $U(s)$:

$$O(s) = U(s)O(0)U^\dagger(s), \tag{7}$$

where $O(0)$ is the bare operator.

B. Momentum projection operator: $a_q^\dagger a_q(k, k')$

Applying $a_q^\dagger a_q(k, k')$ to a wave function $\psi(k)$ returns $\psi(q)$. For the discrete case, $\psi(k_i)$ is an $N \times 1$ vector and $a_q^\dagger a_q(k_i, k_j)$ is an $N \times N$ matrix where $i, j = 1 \cdots N$. Then $a_q^\dagger a_q(k, k')$ acting on $\psi(k)$ is a matrix multiplication, implying a continuous integration over $d^3k/(2\pi)^3 = 2/(\pi k^2 dk)$ in spherical coordinates. Therefore, we include a factor of $\pi/(2k_i k_j \sqrt{w_i w_j})$ in $a_q^\dagger a_q(k_i, k_j)$ where w represents the momentum weights. In matrix form,

$$a_q^\dagger a_q(k_i, k_j) = \frac{\pi \delta_{k_i q} \delta_{k_j q}}{2k_i k_j \sqrt{w_i w_j}}, \tag{8}$$

which has units fm^3. To evolve operators, we apply $U(s)$ at this point. For mesh-independent figures, we must divide by an additional factor of $k_i k_j \sqrt{w_i w_j}$. This operator is inherently mesh-dependent based off discretizing $\delta_{k_i q} \delta_{k_j q}$ above.

C. Momentum distribution function: $\phi^2(k)$

We diagonalize the Hamiltonian for eigenvectors ψ_α. In the ^{3}S$_1$-^{3}D$_1$ coupled channel, the S-component is given by $\psi_\alpha[:N]$ and the D-component by $\psi_\alpha[N:]$ where N is the length of

the momentum mesh. Then the momentum distribution of the state α is given by,

$$|\phi_\alpha(k)|^2 = |\psi_\alpha[:N]|^2 + |\psi_\alpha[N:]|^2. \tag{9}$$

This satisfies the normalization condition $\sum_{i=1}^{N} |\phi(k_i)|^2 = 1$, implying that the factor $k^2 dk$ (or in the discrete case, $k_i^2 w_i$) is factored into the wave function. For mesh-independent figures, divide by $k_i^2 w_i$.

V. CONCLUSION

– Summary.

– Outlook.

[1] F. Wegner, Annalen der Physik **506**, 77 (1994).

[2] P. Reinert, H. Krebs, and E. Epelbaum, Eur. Phys. J. A **54**, 86 (2018), arXiv:1711.08821 [nucl-th].

[3] D. R. Entem and R. Machleidt, Phys. Rev. C **68**, 041001 (2003), arXiv:nucl-th/0304018 [nucl-th].

[4] A. Gezerlis, I. Tews, E. Epelbaum, M. Freunek, S. Gandolfi, K. Hebeler, A. Nogga, and A. Schwenk, Phys. Rev. C **90**, 054323 (2014), arXiv:1406.0454 [nucl-th].

[5] B. Dainton, R. J. Furnstahl, and R. J. Perry, Phys. Rev. C **89**, 014001 (2014), arXiv:1310.6690 [nucl-th].

[6] S. Blanes, F. Casas, J. A. Oteo, and J. Ros, Phys. Rep. **470**, 151 (2009), arXiv:0810.5488 [math-ph].

[7] W. Magnus, Commun. Pure Appl. Math. **7**, 649 (1954).